Available online at www.sciencedirect.com
ScienceDirect
Chemical Physics 332 (2007) 262–270
Chemical Physics
www.elsevier.com/locate/chemphys

Excited and ionized states of ozone studied by the MEG (multi-exponentially generated)/EX (excited)-MEG method

Yuhki Ohtsuka [a], Jun-ya Hasegawa [b], Hiroshi Nakatsuji [a,b,*]

[a] *Fukui Institute for Fundamental Chemistry, Kyoto University, Sakyo-ku, Kyoto 606-8103, Japan*
[b] *Department of Synthetic Chemistry and Biological Chemistry, Graduate School of Engineering, Kyoto University, Nishikyou-ku, Kyoto 615-8510, Japan*

Received 6 September 2005; accepted 8 December 2006
Available online 20 December 2006

Abstract

The MEG (multi-exponentially generated)/EX (excited)-MEG method, which is a multi-reference version of the SAC (symmetry-adapted cluster)/SAC-CI (configuration interaction) method, has been applied to the valence excited and ionized states of ozone that has a quasi-degenerate bi-radical nature in its ground state. The MEG/EX-MEG result shows a remarkable improvement over the single-reference SAC/SAC-CI general-*R* one in both the correlation energy and the ionization potential. The present results were compared with the previous theoretical and experimental data. The theoretical ionization spectrum reproduced the experimental spectrum observed from outer- to inner-valence regions (~28 eV). This is the first report that gives a theoretical interpretation up to a high-energy region.

Keywords: Ozone; Ionized state; Excited state; MEG/EX-MEG; SAC/SAC-CI

1. Introduction

Ozone has attracted many researchers for a long time due to its important photo-chemical and photo-physical roles in the atmospheric ozone layer surrounding the earth. In the electronic spectrum, the four bands, Wulf, Chappius, Huggins and Hartley bands, have been observed in the energy region up to 6 eV [1]. The photo dissociation and recombination processes that are induced through these four excitations are important steps in the atmospheric reactions [1–3], and therefore these photo reactions have received much attention for many years.

The ground state of ozone is characterized as biradical electronic structure. Hartree–Fock (HF) single determinant becomes inadequate approximation due to the quasi-degenerate electronic structure. Therefore, ozone has been a benchmark molecule [4–11] in the methodological developments of the multi-reference type theories in modern quantum chemistry.

Ionization spectra of ozone have also been extensively studied both by experiments [12–18] and theories [4,6,9,19–27]. The quasi-degeneracy in the ground state causes a breakdown of the Koopmans' picture. Many-electron processes that include the excitations to LUMO appear even in the low-lying ionized states. Therefore, multi-reference theories are required for accurate descriptions of the ionized states. For example, a problem in the assignment of the first three peaks had been discussed for many years but seems to have been settled recently [4,6,9,15,22]. However, only qualitative assignments [14,19,20] were given for many correlation peaks that were observed in the higher-energy region of the He II photoelectron spectrum [15].

In addition, the Born–Oppenheimer approximation severely fails in several main bands of both the ionization and excitation spectra, and accurate electronic structures of excited states and the explicit treatment of nuclear dynamics are required for the theoretical account of experiments. Domcke and co-workers investigated the

* Corresponding author. Address: Department of Synthetic Chemistry and Biological Chemistry, Graduate School of Engineering, Kyoto University, Nishikyou-ku, Kyoto 615-8510, Japan.
E-mail address: hiroshi@sbchem.kyoto-u.ac.jp (H. Nakatsuji).

0301-0104/$ - see front matter
doi:10.1016/j.chemphys.2006.12.008

photodissociation in Chappuis band using complete-active-space (CAS) self-consistent field (SCF) and CAS second-order perturbation theory (PT2) wave functions and time-dependent wave-packet calculations, and succeeded in interpretation of very diffuse structure in the spectrum [28–30]. For the two lowest ionized states, Müller et al. reproduced the vibronic structure in the spectrum using CASSCF and multi-reference (MR) CI wave functions and a multi-mode vibronic coupling Hamiltonian [26,27].

We have studied excited and ionized states of many molecular systems using the SAC (symmetry adapted cluster) [31]/SAC-CI (configuration interaction) [32] method [33–35] and showed that the SAC-CI method is able to reproduce the experimental spectra in wide energy regions [35]. An advantage of the SAC-CI method is that it can describe many different kinds of excited states simultaneously in a similar accuracy. Therefore, the SAC-CI method is very useful for studying many different kinds of spectroscopies. However, since the SAC method is a single-reference theory, the SAC-CI method may loose its reliable accuracy when the HF single determinant approximation becomes inadequate [36]. Such situation would certainly occur in ozone for its quasi-degenerate nature of the ground state and also generally in the near-dissociation limits of homopolar chemical bonds. To overcome this difficulty, the MEG4 (multi-exponentially generated 4th)/EX (excited)-MEG4 method was proposed [37] as a generalization of the SAC/SAC-CI method to the multi-reference case. In The MEG4/EX-MEG4 method, non-separable (static) correlations which require multi-reference description are expressed by exponentially generated (EG) CI [38,39]. The MEG4/EX-MEG4 method has been applied to the potential energy surfaces of small molecules in their ground and excited states and reproduced the full-CI energy within a error of a few milli-hartrees [37].

In this article, we describe the applications of the MEG4/EX-MEG4 method to the singlet and triplet excited states and the ionized states of ozone, and discuss the accuracy and the applicability of the MEG4/EX-MEG4 method. The ionization spectrum of ozone up to 28 eV is assigned and compared with the previous theoretical assignments. We also compare the MEG4/EX-MEG4 result with the SAC/SAC-CI one, to evaluate the effect of the multi-reference.

2. Computational details

We calculated vertical excitation and ionization energies using the experimental C_{2v} geometry [40] for the ground state of ozone. The O–O bond length and the O–O–O angle are 1.272 Å and 116.8°, respectively. The basis set used was TZ (Dunning) [5s3p] [41] set augmented with the Rydberg basis (1s1p)/[1s1p] for 3s and 3p orbitals on each atom. The total number of bases was 54. The active space in the EGCI, MEG4 and EX-MEG4 calculations consists of 9 occupied and 39 virtual orbitals. Three 1s and the corresponding virtual MO's were frozen. The number of solutions was 3 for each symmetry in the singlet and triplet states, and 15 for each symmetry in the ionized states. The perturbation selection [42] was carried out for the linked operators, $\widehat{S}_I^\dagger$ and $\widehat{E}_K^\dagger$ in Eqs. (14) and (21) of Ref. [37]. For the ground state, the HF determinant was used as the reference for the selection. To obtain reference configurations for the excited and ionized states, preliminary SD-CI calculations within a small active space (9 occ. × 15 vir.) were performed, and we selected single and double excitations having the coefficients larger than 0.1 for selecting double excitations. Using these reference configurations, the perturbation selection was carried out with the energy thresholds of 1×10^{-5} and 1×10^{-6} (a.u.) for the ground and excited (ionized) states, respectively. For the unlinked operators, all linked operators having coefficients larger than 0.05 were included.

The ionization cross-sections were calculated using the monopole approximation [43,44] to estimate the relative intensities of the peaks in the ionization spectrum. For calculating the monopole intensities, the MEG4 wave function was used for the ground state. To compute the excitation energy and ionization potentials (IPs), the ground state energy calculated by the EX-MEG4 method was used.

The Hartree–Fock calculation was performed using HONDO95 program [45]. The SAC/SAC-CI and the MEG4/EX-MEG4 calculations were performed with a development version of the program system for the EGWF and EX-EGWF methods [46].

3. Results and discussion

3.1. Ground state

The Hartree–Fock electronic configuration for the ground state of ozone is written as

$$(\text{core})(4a_1)^2(5a_1)^2(3b_2)^2(1b_1)^2(4b_2)^2(6a_1)^2(1a_2)^2(2b_1)^0.$$

The orbitals, $1b_1$, $1a_2$ and $2b_1$ are out-of-plane π orbitals with bonding, non-bonding, and antibonding characters, respectively. The $5a_1$, $4b_2$, and $6a_1$ are in-plane π orbitals with bonding, non-bonding, and antibonding characters, respectively. The $3b_2$ orbital has σ antibonding character.

First, we examine the ground state correlation energy that is dependent on the reference function. All calculations employed the same excitation operators, $\widehat{S}_I^\dagger$ and $\widehat{E}_K^\dagger$ for the MEG4 and EX-MEG4 wave functions. Therefore, the only difference is in the reference function, Φ_0 in Eq. (16) of Ref. [37].

In Table 1, the results of the MEG4/EX-MEG4 method for the ground state are summarized. The MEG4 (1 Ref.) and EX-MEG4 (1 Ref.) wave functions, which have single reference function (HF determinant) in Φ_0, are identical to the SAC and SAC-CI general-R wave functions, respectively. In the MEG4 (2 Ref.) wave function, a double excitation $(\text{HOMO})^2 \rightarrow (\text{LUMO})^2$ is also included in the reference function Φ_0. As seen in Table 1, the MEG4 (1 Ref.) calculation is insufficient, and the MEG4 (2 Ref.)

Table 1
Singlet and triplet states of ozone calculated by the MEG4/EX-MEG4 method

State	Exptl.[a]	MEG4/EX-MEG4			
		1 Ref.[b]	2 Ref.[c]	3 Ref.[d]	
	EE(eV)	EE(eV)	EE(eV)	EE(eV)	Main configuration ($C > 0.2$)
Singlet states					
X^1A_1 MEG4[e]		(−0.41255)	(−0.42216)	(−0.42454)	$-0.92(\mathrm{HF}) + 0.37((1a_2)^2 \rightarrow (2b_1)^2)$
EX-MEG4[e]		(−0.44837)	(−0.44915)	(−0.45264)	$-0.87(\mathrm{HF}) + 0.27((1a_2)^2 \rightarrow (2b_1)^2)$
2^1A_1		4.25	4.28	4.38	$-0.74((6a_1)^2 \rightarrow (2b_1)^2) + 0.51((4b_2)^2 \rightarrow (2b_1)^2) + 0.23(4b_2, 3b_2 \rightarrow (2b_1)^2)$
1^1A_2	~1.6	2.15	2.18	2.21	$-0.74(4b_2 \rightarrow 2b_1) + 0.52(1a_2, 6a_1 \rightarrow (2b_1)^2)$
1^1B_1	2.1	2.06	2.08	2.18	$-0.82(6a_1 \rightarrow 2b_1) + 0.46(4b_2, 1a_2 \rightarrow (2b_1)^2)$
1^1B_2	4.9	5.11	5.16	5.27	$0.80(1a_2 \rightarrow 2b_1) - 0.45(1a_2, 1b_1 \rightarrow (2b_1)^2)$
Triplet states					
1^3A_2	–	1.95	1.97	2.07	$-0.83(4b_2 \rightarrow 2b_1) + 0.43(1a_2, 6a_1 \rightarrow (2b_1)^2)$
1^3B_1	–	1.65	1.67	1.77	$0.86(6a_1 \rightarrow 2b_1) - 0.38(4b_2, 1a_2 \rightarrow (2b_1)^2)$
1^3B_2	–	1.67	1.71	1.78	$-0.96(1a_2 \rightarrow 2b_1)$

[a] Ref. [1].
[b] Identical to the SAC/SAC-CI general-R method.
[c] Reference function is $0.94(\mathrm{HF}) - 0.34((1a_2)^2 \rightarrow (2b_1)^2)$.
[d] Reference function is $-0.92(\mathrm{HF}) + 0.37((1a_2)^2 \rightarrow (2b_1)^2) - 0.12((1b_1) \rightarrow (2b_1))$.
[e] For the X^1A_1 ground state (MEG4 and EX-MEG4), the correlation energy in a.u. is shown in the parentheses. For the other states, X^1A_1 state (EX-MEG4) was used for the ground state to calculate the excitation energy (EE).

result improves about 10 mhartree in the correlation energy. In the MEG4 (2 Ref.) wave function, the cluster amplitude c_I for $(\mathrm{HOMO})^2 \rightarrow (\mathrm{LUMO})^2$ is 0.1, which is smaller than that in the SAC wave function (0.2). This decrease is due to the fact that the effect of this double excitation is already taken into account by the MR-part of the wave function. Third important operator, $1b_1$ (out-of-plane π orbital) → LUMO, was also included in the MR-part of MEG4 (3 Ref.). However, the difference from the MEG4 (2 Ref.) result is only about 2 mhartree, showing that the multi-reference effect is almost saturated at the MEG4 (2 Ref.) level of calculation.

Next, we compare the EX-MEG4 result for the ground state with the MEG4 one. In the MEG4 wave function, the $S_I^\dagger$ operators are defined as single and double excitations from the HF determinant, not from all the reference functions. This was also pointed by Hirao [47]. However, the effect of the neglected operators is included in the EX-MEG4 wave function as the excitations higher than doubles in the $\widehat{E}_K^\dagger$ operator. As shown in Table 1, this improves considerably the ground state energy of ozone. The EX-MEG4 method gave larger correlation energy than the MEG4 method in all calculations and the calculated correlation energy was almost independent of the number of the reference functions. Together with the exp operators that mainly describe the ground state dynamical correlations, the $\widehat{E}_K^\dagger$ operators take into account both of the non-dynamical and the remaining dynamical correlations in a balanced way.

Total energies by the MEG4 and EX-MEG4 methods are −224.66841 and −224.69651 a.u. using Dunning TZ + Rydberg [1s1p] basis sets, and −224.83023 and −224.84703 a.u. using cc-pVDZ basis sets [48], respectively. Despite smaller basis sets and less configuration state functions (CSFs) used in our calculations, these values are lower than the MC-SCF results −224.66625 (QZVP + Rydberg (Uncontracted)), −224.62019 (QZVP + Rydberg), and −224.62221 (TZVP) a.u. [24] due to the dynamical correlations introduced by the MEG4 method. However, they are higher than some MRD-CI results −225.08975 (van Duijneveldt (13s8p)/[8s5p] + Pol. [2d1f]) [25] and −224.97656 a.u. (Dunning (9s5p)/[5s3p] + diff. [1s1p] + Bond pol. [1s1p]) [49]. In MRD-CI method, extrapolations after solving secular equations are supposed to make the total energies lower. To our knowledge the MRMP method gave the lowest energy −225.0954 a.u. so far using the cc-pVTZ basis set augmented with the diffuse functions (1s1p1d) [8].

3.2. Ionized states

The ionized states of ozone calculated by the EX-MEG4 method and the SAC-CI general-R method are summarized in Table 2. The theoretical ionization spectrum is compared with a He II photoelectron spectrum [15] in Fig. 1. The experimental spectrum shown in Fig. 1 covers the widest energy range in the spectra so far reported. The full width at half-maximum (FWHM) of the calculated monopole intensities was set to 0.4 eV for all the computed ionized states. For calculating the ionized states, two-reference functions was used in the MR part Φ_0, since the MEG4 correlation energy seemed to converge at the 2-reference level, as discussed above.

With regard to the first three intense peaks at 12.7, 13.0, and 13.5 eV, there are many theoretical [4,6,9,19–27] and experimental [12–18] studies. From the Koopmans' theorem, these three peaks are assigned to 1^2A_2, 1^2A_1, and 1^2B_2 states, respectively. However, the Koopmans' approximation breaks down for ozone, since the Hartree–Fock single determinant is not an adequate approximation due to the quasi-degeneracy in the ground state. Initial state effects play an important role for the correct order of the

Table 2
Ionization potential(eV), monopole intensity, and main configuration of the ionized states of ozone

State	Exptl.[a]	SAC-CI	EX-MEG4[b]	
	I.P.(Peak)[c]	I.P.	I.P.(Intensity)[c]	Main configuration ($C > 0.3$)
1^2A_1	12.73(1)	13.12	12.98(0.671)	$0.80(6a_1^{-1}) - 0.33(1a_2^{-2}2b_1^2 6a_1^{-1})$
1^2B_2	13.00(2)	13.36	13.29(0.621)	$0.78(4b_2^{-1}) - 0.33(1a_2^{-1}2b_1 6a_1^{-1})$
1^2A_2	13.54(3)	13.78	13.79(0.705)	$-0.90(1a_2^{-1})$
1^2B_1		14.65	$14.66(8.0\times10^{-5})$	$-0.72(6a_1^{-2}2b_1) + 0.52(4b_2^{-2}2b_1)$
2^2A_2		15.10	$15.12(5.0\times10^{-5})$	$0.59(4b_2^{-1}2b_1 6a_1^{-1}) - 0.45(6a_1^{-1}2b_1 4b_2^{-1})$ $-0.37(4b_2^{-1}1b_1^{-1}2b_1^2 6a_1^{-1})$
2^2B_2	15.6(A)	15.59	15.63(0.0103)	$0.82(6a_1^{-1}2b_1 1a_2^{-1}) + 0.32(1a_2^{-1}2b_1 6a_1^{-1})$
2^2A_1		16.20	16.24(0.00263)	$-0.80(4b_2^{-1}2b_1 1a_2^{-1})$
2^2B_1	16.50(4)	16.86	16.75(0.139)	$-0.80(1a_2^{-2}2b_1) + -0.34(1b_1^{-1})$
3^2A_2		17.18	17.21(0.00166)	$-0.60(6a_1^{-1}2b_1 4b_2^{-1}) - 0.51(4b_2^{-1}2b_1 6a_1^{-1}) - 0.35(6a_1^{-2}2b_1^2 1a_2^{-1})$
3^2B_1	17.6(5)	17.78	17.78(0.0227)	$0.61(4b_2^{-2}2b_1) + 0.45(6a_1^{-2}2b_1) + 0.36(6a_1^{-1}4b_2^{-1}2b_1^2 1a_2^{-1})$
3^2A_1	17.6(5)	17.95	17.88(0.180)	$0.56(1a_2^{-1}2b_1 4b_2^{-1}) - 0.39(5a_1^{-1}) - 0.37(1a_2^{-2}2b_1^2 6a_1^{-1}) + 0.30(1a_2^{-1}4b_2^{-1}2b_1^2 1b_1^{-1})$
3^2B_2	17.6(5)	18.29	18.25(0.0950)	$-0.58(1a_2^{-1}2b_1 6a_1^{-1}) + 0.34(1a_2^{-2}2b_1^2 4b_2^{-1}) - 0.31(1a_2^{-1}6a_1^{-1}2b_1^2 1b_1^{-1})$
4^2B_2	19.4(6)	18.94	18.97(0.00651)	$-0.78(6a_1^{-2}2b_1^2 4b_2^{-1}) - 0.30(4b_2^{-1}5a_1^{-1}2b_1^2 6a_1^{-1})$
4^2A_2		19.50	19.52(0.0)	$-0.50(6a_1^{-2}2b_1^2 1a_2^{-1}) + 0.46(4b_2^{-2}2b_1^2 1a_2^{-1}) + 0.34(4b_2^{-1}2b_1 6a_1^{-1})$
4^2B_1		19.48	$19.52(6.0\times10^{-5})$	$0.77(1a_2^{-1}6a_1^{-1}2b_1^2 4b_2^{-1}) + 0.38(6a_1^{-1}4b_2^{-1}2b_1^2 1a_2^{-1})$
4^2A_1	20.0(6)	19.98	20.01(0.0745)	$0.71(4b_2^{-2}2b_1^2 6a_1^{-1})$
5^2B_2	20.0(6)	20.18	20.14(0.144)	$0.49(4b_2^{-1}2b_1 1b_1^{-1}) - 0.46(5a_1^{-1}2b_1 1a_2^{-1}) - 0.36(3b_2^{-1})$
5^2A_1	20.0(6)	20.39	20.16(0.189)	$0.39(5a_1^{-1}) - 0.32(4b_2^{-2}11a_1) + 0.32(6a_1^{-2}11a_1)$
6^2B_2	20.0(6)	20.74	20.57(0.379)	$0.59(3b_2^{-1}) - 0.36(5a_1^{-1}2b_1 1a_2^{-1}) + 0.34(4b_2^{-1}2b_1 1b_1^{-1})$
5^2A_2		21.31	21.33(0.0)	$-0.52(1a_2^{-1}6a_1^{-1}2b_1^2 5a_1^{-1}) - 0.49(4b_2^{-1}1b_1^{-1}2b_1^2 6a_1^{-1}) - 0.35(5a_1^{-1}2b_1 4b_2^{-1})$
5^2B_1	20.8(6)	21.64	21.44(0.354)	$0.56(1b_1^{-1}) + 0.52(1a_2^{-2}2b_1) - 0.30(1a_2^{-2}2b_1^2 1b_1^{-1})$
6^2A_1	20.8(6)	21.45	21.61(0.0288)	$0.37(1a_2^{-2}2b_1^2 6a_1^{-1}) + 0.35(4b_2^{-1}1b_1^{-1}2b_1^2 1a_2^{-1}) + 0.31(6a_1^{-1}2b_1 1b_1^{-1})$
6^2B_1		21.87	21.89(0.00328)	$-0.57(6a_1^{-1}4b_2^{-1}2b_1^2 1a_2^{-1}) - 0.33(3b_2^{-1}2b_1 4b_2^{-1}) + 0.33(4b_2^{-1}3b_2^{-1}2b_1^2 1a_2^{-1})$
7^2A_1	20.8(6)	22.06	22.06(0.0181)	$0.40(1b_1^{-1}2b_1 6a_1^{-1}) - 0.39(6a_1^{-2}11a_1) + 0.30(6a_1^{-1}2b_1 1b_1^{-1})$
7^2B_2		21.99	22.10(0.00203)	$0.46(1a_2^{-2}2b_1^2 4b_2^{-1}) - 0.38(1b_1^{-1}2b_1 4b_2^{-1})$
8^2A_1	20.8(6)	22.44	22.26(0.0935)	$-0.52(6a_1^{-2}11a_1) + 0.30(6a_1^{-1}2b_1 1b_1^{-1})$
7^2B_1		22.48	$22.35(2.7\times10^{-4})$	$-0.55(4b_2^{-1}2b_1 3b_2^{-1}) + 0.30(5a_1^{-1}2b_1 6a_1^{-1}) - 0.30(1a_2^{-1}6a_1^{-1}2b_1^2 4b_2^{-1})$
6^2A_2		22.41	$22.44(1.0\times10^{-4})$	$-0.40(4b_2^{-2}2b_1^2 1a_2^{-1}) - 0.38(3b_2^{-1}2b_1 6a_1^{-1}) + 0.32(6a_1^{-1}5a_1^{-1}2b_1^2 1a_2^{-1})$
7^2A_2		22.69	$22.63(3.9\times10^{-4})$	$0.52(6a_1^{-1}2b_1 3b_2^{-1}) + 0.36(1a_2^{-1}11a_1 6a_1^{-1}) - 0.35(1a_2^{-1}4b_2^{-1}2b_1^2 3b_2^{-1})$
8^2A_2		22.90	22.92(0.00118)	$0.54(1a_2^{-1}11a_1 6a_1^{-1}) - 0.43(6a_1^{-1}2b_1 3b_2^{-1})$
8^2B_2	22.7(B)	23.20	23.03(0.0211)	$0.62(6a_1^{-1}11a_1 4b_2^{-1})$
9^2A_1	22.7(B)	23.12	23.11(0.0402)	$-0.70(3b_2^{-1}2b_1 1a_2^{-1}) - 0.37(1a_2^{-1}2b_1 3b_2^{-1})$
9^2A_2		23.13	$23.16(8.3\times10^{-4})$	$-0.62(6a_1^{-1}11a_1 1a_2^{-1}) - 0.41(1a_2^{-1}11a_1 6a_1^{-1})$
8^2B_1		23.18	$23.20(1.7\times10^{-4})$	$0.53(1a_2^{-1}11a_1 4b_2^{-1})$
9^2B_2		23.42	23.44(0.00363)	$-0.50(5a_1^{-1}2b_1 1a_2^{-1}) - 0.41(4b_2^{-1}2b_1 1b_1^{-1})$
9^2B_1		23.46	23.54(0.00619)	$-0.50(6a_1^{-1}2b_1 5a_1^{-1}) - 0.36(5a_1^{-1}2b_1 6a_1^{-1})$
10^2B_2		23.97	23.83(0.00247)	$-0.49(4b_2^{-1}11a_1 6a_1^{-1}) - 0.45(11a_1^{-2}9b_2)$
10^2A_1		24.16	24.10(0.00385)	$-0.48(4b_2^{-2}11a_1) + 0.40(1a_2^{-2}11a_1)$
10^2A_2	24.1(C)	24.43	24.49(0.00674)	$0.44(1b_1^{-1}2b_1 1a_2^{-1}) - 0.32(6a_1^{-1}5a_1^{-1}2b_1^2 1a_2^{-1}) + 0.31(1a_2^{-1}2b_1 1b_1^{-1})$
11^2B_2	24.1(C)	25.09	24.77(0.0115)	$0.42(4b_2^{-2}9b_2) + 0.33(6a_1^{-1}11a_1 2b_1 1a_2^{-1})$
11^2A_1	24.1(C)	24.77	24.94(0.0300)	$0.65(1a_2^{-2}11a_1)$
10^2B_1		24.38	$25.03(3.9\times10^{-4})$	$-0.48(3b_2^{-1}2b_1 4b_2^{-1}) - 0.38(1a_2^{-1}6a_1^{-1}2b_1^2 4b_2^{-1})$
12^2B_2		25.28	25.16(0.00115)	$-0.46(1b_1^{-1}2b_1 4b_2^{-1}) + 0.40(1a_2^{-1}2b_1 5a_1^{-1}) - 0.32(1a_2^{-1}6a_1^{-1}2b_1^2 1b_1^{-1})$
12^2A_1	24.1(C)	25.09	25.16(0.0518)	$-0.44(1a_2^{-1}2b_1 3b_2^{-1}) + 0.44(1a_2^{-2}11a_1) + 0.35(1b_1^{-1}2b_1 6a_1^{-1})$
11^2A_2		25.52	25.42(0.0)	$-0.53(3b_2^{-1}2b_1 6a_1^{-1})$
13^2A_1		25.51	25.47(0.00363)	$-0.60(4b_2^{-1}9b_2 6a_1^{-1})$
11^2B_1		25.97	$26.00(1.7\times10^{-4})$	$-0.65(1a_2^{-1}9b_2 6a_1^{-1}) - 0.31(6a_1^{-1}9b_2 1a_2^{-1})$
12^2A_2		–[d]	26.60(0.0037)	$-0.42(1a_2^{-1}9b_2 4b_2^{-1}) + 0.41(1a_2^{-1}2b_1 1b_1^{-1})$
13^2B_2		–[d]	$26.62(3.0\times10^{-4})$	$0.50(6a_1^{-2}11a_1 2b_1 1a_2^{-1}) - 0.30(4b_2^{-2}9b_2)$
14^2B_2		27.03	27.07(0.00121)	$-0.72(1a_2^{-2}9b_2) - 0.30(1a_2^{-1}11a_1 1b_1^{-1})$
13^2A_2		27.20	27.15(0.00202)	$-0.62(4b_2^{-1}9b_2 1a_2^{-1}) - 0.31(1a_2^{-1}9b_2^{-1}4b_2^{-1})$
14^2A_1	26.8(D)	27.13	27.23(0.124)	$0.34(4a_1^{-1})$
14^2A_2		27.78	$27.40(3.6\times10^{-4})$	$-0.38(1a_2^{-1}9b_2 4b_2^{-1}) - 0.36(4b_2^{-1}9a_1 1b_1^{-1}) - 0.36(1b_1^{-1}11a_1 4b_2^{-1}) + 0.33(4b_2^{-1}1a_2^{-2}11a_1 2b_1)$
15^2A_1	26.8(D)	27.78	27.54(0.0151)	$0.66(4b_2^{-1}1b_1^{-1}2b_1^2 1a_2^{-1})$
15^2A_2		27.67	$27.67(2.6\times10^{-4})$	$0.40(1b_1^{-1}11a_1 4b_2^{-1}) - 0.33(1a_2^{-1}9b_2 4b_2^{-1}) - 0.31(4b_2^{-1}11a_1 1b_1^{-1})$
12^2B_1		–[d]	$28.22(1.3\times10^{-4})$	$0.58(1b_1^{-1}11a_1 6a_1^{-1}) - 0.30(6a_1^{-1}11a_1 1b_1^{-1})$
13^2B_1		–[d]	$28.80(2.0\times10^{-5})$	$0.60(1b_1^{-1}11a_1 6a_1^{-1})$

[a] Ref. [15].
[b] Two reference functions, $0.94(\mathrm{HF}) - 0.34((1a_2)^2 \rightarrow (2b_1)^2)$, are used for the MEG4/EX-MEG4 calculation.
[c] I.P.s were calculated from the ground state calculated by the EX-MEG4 method.
[d] No corresponding solutions were found.

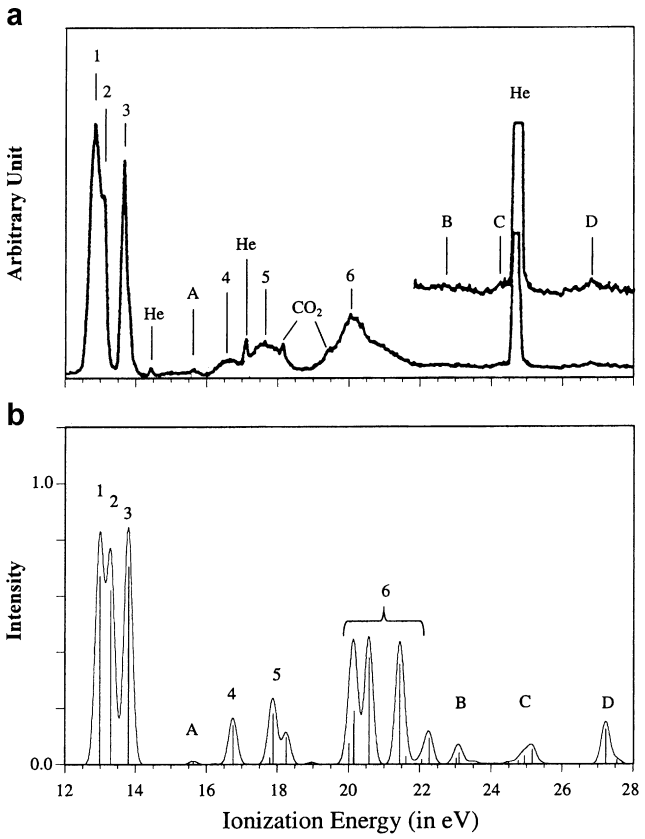

Fig. 1. (a) He II photoelectron spectrum of ozone[15], and (b) theoretical ionization spectrum calculated by the MEG4/EX-MEG4 method. In the theoretical spectrum, the calculated pole strength is shown by the solid vertical lines at each ionization potential, and the Gaussian curves are drawn with the averaged line width (0.4 eV FWHM).

lowest three ionized states as discussed using valence bond picture by Kosugi et al. [22]. Therefore, the EX-MEG4 calculation gave the different order from Koopmans' theorem: 1^2A_1 (12.98 eV) < 1^2B_2 (13.29 eV) < 1^2A_2 (13.79 eV). The calculated IPs showed reasonable agreement with the experimental data, 12.73, 13.00, and 13.54, respectively [12–18]. The theoretical ionization spectrum reproduced well the experimental one, as shown in Fig. 1. This assignment is the same as that reported in the previous studies [4,6,9,14,15,20,22–25], as summarized in Table 3. The main configurations of the 1^2A_1, 1^2B_2, and 1^2A_2 states are one-electron ionizations from the $6a_1$ (in-plane π antibonding), $4b_2$ (in-plane π non-bonding), and $1a_2$ (out-of-plane π non-bonding, HOMO) orbitals, respectively. However, for the 1^2A_1 and 1^2B_2 states, three-electron processes mix strongly with the one-electron ionizations. These configurations are characterized as the one-electron ionization $(6a_1)^{-1}$ from the doubly excited configuration, $(1a_2, \text{HOMO})^2 \rightarrow (2b_1, \text{LUMO})^2$, as shown in Table 2, which reflects the quasi-degeneracy in the ground state.

The EX-MEG4 results are also compared with the SAC-CI general-*R* ones in Table 2. In contrast to the former subsection, the improvements were obtained by the multi-reference projection space: $(\text{HOMO})^2 \rightarrow (\text{LUMO})^2$ excitation included in the projection space $\langle \Phi_0|$ in Eq. (22) of Ref. [37]. It is seen that IPs were especially improved in the ionized states dominated by one-electron processes, 1^2A_1, 1^2B_2, 3^2A_1, 5^2A_1, 14^2A_1, 5^2B_1, and 6^2B_2 states, and their IPs were reduced by 0.07–0.23 eV. For example, the IPs for the 1^2A_1 and 1^2B_2 states were reduced by about 0.1 eV due to the EX-MEG4 method and became closer to the experimental IPs. On the other hand, there are two cases where the IPs calculated by the EX-MEG4 and SAC-CI general-*R* methods were very close to each other. The first one is the ionization from HOMO (1^2A_2 state), and the second one is the two-electron process including the excitation to LUMO. A possible reason is that the projection space, $\langle \Phi_0|$, which consists of an EGCI expansion, gave only small effect. Although the reference function includes the double excitation from HOMO to LUMO, $\widehat{G}^{aa}_{ii}$ in Eq. (13) of Ref. [37], this operator has no effect to the equation, if the ionization operator $\widehat{E}_i$ that removes an electron from HOMO, or $\widehat{E}^a_{jk}$ that adds an electron to

Table 3
Vertical ionization energy (eV) of ozone calculated by the MEG4/EX-MEG4 method and other theoretical methods

State	MEG4/EX-MEG4[a]	Exptl.[c]	Previous theoretical studies						
	2 Ref.[b]		MRD-CI[d]	FSMRCC[e]	GVB-CI[f]	MCSCF + CI[g]	MCSCF + CI[h]	MRCI[i]	MCSTEP[j]
1^2A_1	12.98	12.73	12.46	12.69	12.91	12.53	12.40	12.44	12.87
1^2B_2	13.29	13.00	12.53	12.82	13.03	13.09	12.79	12.49	13.16
1^2A_2	13.79	13.54	13.05	13.43	13.59	12.81	12.97	13.17	13.53
2^2B_2	15.63	15.6				19.02			
2^2B_1	16.75	16.54	16.37		16.67	15.91			

[a] Dunning TZ + Ryd[1s1p] (each atom).
[b] Reference function is 0.94(HF) − 0.34 $((1a_2)^2 \rightarrow (2b_1)^2)$.
[c] Ref. [15].
[d] Ref. [4]. Dunning (10s5p)/[4s2p] + Ryd. [1s1p] (central oxygen) + Bond pol. [1s] (each bond).
[e] Ref. [6]. [14s7p3d/5s4p2d] basis set.
[f] Ref. [20]. DZ basis set.
[g] Ref. [19]. DZ basis set.
[h] Ref. [24]. TZVP.
[i] Ref. [25]. van Duijneveldt (13s8p)/[8s5p] + Dunning [2d1f].
[j] Ref. [9]. CBS.

LUMO, was multiplied. In both cases, the projection space becomes qualitatively equivalent to that of the SAC-CI general-R as follows:

$$\langle \Phi_0|\widehat{E}_i = \langle 0|(g_0 + g^{aa}_{ii}\widehat{G}^{aa}_{ii})\widehat{E}_i = g_0\langle 0|\widehat{E}_i, \quad (1)$$

$$\langle \Phi_0|\widehat{E}^a_{jk} = \langle 0|(g_0 + g^{aa}_{ii}\widehat{G}^{aa}_{ii})\widehat{E}^a_{jk} = g_0\langle 0|\widehat{E}^a_{jk}, \quad (2)$$

where the indices i and a represent HOMO and LUMO, respectively, and j and k are arbitrary occupied orbitals. These results show that the EX-MEG4 method is useful for describing ionized states when initial state effects are important. It is interesting that the strong peaks observed in the spectrum show large improvements by the present multi-reference treatment.

A weak band A at 15.6 eV (hereafter, we conform the peak notations used in Ref. [15]) was assigned to 2^2B_2 state with the calculated IP of 15.63 eV, which supports the previous proposal [22]. As shown in Table 3, a pioneering MCSCF-CI calculation [19] performed in 1975 overestimated the IP for the 2^2B_2 state. Due to the present calculation, the 2^2B_2 state is characterized as a satellite peak of the 1^2B_2 state and the main configuration is a two-electron process represented by ($6a_1^{-1}2b_1 1a_2^{-1}$) (see Table 2).

The peak 4 at 16.50 eV was assigned to 2^2B_1 state calculated at 16.75 eV. The main configuration was dominated by the two-electron process ($1a_2^{-2}2b_1$) and the intensity was borrowed from the ionization from the $1b_1$ orbital (out-of-plane π bonding). This assignment agrees with that reported in Refs. [4,20,22]. The parent peak of the peak 4 (2^2B_1 state) is actually in the higher energy region: a broad shoulder in the higher-energy side of the peak 6 (5^2B_1 state shown in Table 2).

A broad peak 5 which has the peak maximum at 17.6 eV was assigned to a composite of the 3^2B_1, 3^2A_1 and 3^2B_2 states with the calculated IPs of 17.78, 17.88 and 18.25, respectively. The 3^2B_1 state has a relatively small intensity (0.0227) and can be ascribed to a shoulder in the low-energy side. The 3^2A_1 and 3^2B_2 states have relatively large intensities (0.180 and 0.095, respectively) and, therefore, can be assigned to the peak maximum and the higher-side shoulder, respectively. All of these three states are due to the two-electron processes, as shown in Table 2. The 3^2A_1 state would correspond to one of the main peaks of the ionization from the $5a_1$ orbital (in-plane π bonding), though the intensity was rather small as a main peak. The intensity contribution from the $5a_1^{-1}$ configuration splits mainly into other three states, 4^2A_1, 5^2A_1, and 8^2A_1 states, as seen from Table 2.

As seen in Fig. 1, a rather strong peak labeled 6 starts from around 19 eV, and has a maximum and a broad shoulder at 20.0 and 20.5–22.0 eV, respectively. In the experiment [15], the peak 6 was assigned as a composite of three absorptions: a shoulder at 19.4, a peak at 20.0, and a shoulder at 20.8 eV. Contamination of CO_2 peak was also implied, which gave a small peak at around 19.5 eV [15]. In this energy region, we obtained many states as shown in Table 2. The 4^2B_2 state calculated at 18.97 eV can be ascribed to the onset of the peak 6, although the peak of CO_2 appears in this region. The main configuration of the 4^2B_2 state is three-electron process which is characterized as one-electron ionization, $4b_2^{-1}$, from the $(6a_1)^2$-$(LUMO)^2$ configuration. For the absorption around the peak maximum, we assigned four states, 4^2A_1, 5^2B_2, 5^2A_1, and 6^2B_2, which have relatively large intensities (0.075, 0.144, 0.189, and 0.379, respectively). The 4^2A_1 state is due to the three-electron process and its intensity originates from $5a_1^{-1}$ configuration. The 5^2B_2 state is due to the two-electron process and its intensity originates from $3b_2^{-1}$ configuration (ionization from σ antibonding MO). The 5^2A_1 state is characterized as a linear combination of ($5a_1^{-1}$) and the two-electron processes including Rydberg excitations, ($4b_2^{-2}11a_1$) and ($6a_1^{-2}11a_1$), where $11a_1$ is 3s orbital. Together with the 3^2A_1 state, the 4^2A_1, 5^2A_1 and 8^2A_1 states are characterized as the correlation peaks that originate from $5a_1^{-1}$ configuration. The 6^2B_2 state, which has the largest intensity in peak 6, is dominated by the single ionization from $3b_2$ orbital. The large shoulder in the higher-energy side of peak 6 is assigned to the 5^2B_1 state. This state is characterized as the one-electron ionization from $1b_1$ (out-of-plane π bonding) orbital. The 6^2A_1, 7^2A_1, and 8^2A_1 states have intensities 0.0228, 0.0181, and 0.0935, respectively, that also contribute to the tail of peak 6 and the latter two states include excitations to the Rydberg orbitals. As shown in Table 2, there are other states with very small intensities, 4^2A_2(19.52 eV), 4^2B_1(19.52 eV), 5^2A_2(21.33 eV), 6^2B_1(21.89 eV), 7^2B_2(22.10 eV), 7^2B_1 (22.35 eV), and 6^2A_2(22.44 eV). As a result, the intensities of peak 6 were mainly obtained by the ionizations from $5a_1$ (in-plane π bonding), $3b_2$(σ antibonding), and $1b_1$ (out-of-plane π bonding) orbitals.

The experiment suggested the existence of the extremely small peaks, B (22.7 eV), C (24.1 eV), and D (26.8 eV) in the higher-energy region of peak 6 [15]. As described by the experimental paper [15], it would be difficult to interpret these peaks only from the experimental data. In our calculations, we got many peaks as shown in Fig. 1. For peak B, 8^2B_2 (23.03 eV) and 9^2A_1 (23.11 eV) states can be assigned, since other states in this energy region, 7^2A_2 (22.63 eV), 8^2A_2 (22.92 eV), 9^2A_2 (23.16 eV), 8^2B_1 (23.20 eV), 9^2B_2 (23.44 eV), and 9^2B_1 (23.54 eV) have very small intensities. The peak C can be interpreted to be 10^2A_2, 11^2B_2, 11^2A_1, and 12^2A_1 states at 24.49, 24.77, 24.94, and 25.16 eV, respectively. However, 11^2A_1, and 12^2A_1 states may be covered with the higher-side of the strong He peak observed next to the peak C.

For the peak D, the 14^2A_1 and 15^2A_1 state at 27.23 and 27.54 eV, respectively, can be the candidates. The 14^2A_1 state has large intensity due to the single ionization nature from the $4a_1$ orbital, which has 2s antibonding character. The 15^2A_1 state is dominated by the three-electron process, ($4b_2^{-1}1b_1^{-1}2b_1^2 1a_2^{-1}$). Other states around peak D have very small intensities. The 13^2A_1 (25.47 eV), 11^2B_1 (26.00 eV), 12^2A_2 (26.60 eV), 14^2B_2 (27.07 eV), and 14^2A_2 (27.40 eV) states are characterized as the two-electron processes

including the excitations to the $9b_2$ orbital, which has 3s and 3pσ characters.

Although we got the states corresponding to all peaks observed, the calculation using the basis sets larger than the current basis set (Dunning TZ + Rydberg basis [1s1p]) would be required to verify the present assignment.

3.3. Vertical singlet and triplet valence excited states

Table 1 summarizes the vertical excitation energies and the main configurations of the valence singlet and triplet states calculated by the EX-MEG4 method. To compute excitation energy, the X^1A_1 state obtained by the EX-MEG4 method was used as the ground state. The excitation energies for the three triplet states, 1^3A_2, 1^3B_1 and 1^3B_2, were calculated at 2.07, 1.77, and 1.78 eV, respectively, with the EX-MEG4 (3 Ref.) calculations. The main configurations of the 1^3A_2, 1^3B_1, and 1^3B_2 states are single excitation to LUMO: $4b_2 \rightarrow 2b_1$, $6a_1 \rightarrow 2b_1$, and $1a_2(\text{HOMO}) \rightarrow 2b_1$, respectively. For the 1^3A_2 and 1^3B_1 states, double excitations to LUMO mix significantly, as shown in Table 1. The singlet excited states are calculated to have higher excitation energies than the three triplet states. The vertical excitation energies for 1^1A_2, 1^1B_1, 1^1B_2, and 2^1A_1 states were calculated at 2.21, 2.18, 5.27, and 4.38 eV, respectively. The main configurations of the 1^1A_2, 1^1B_1, and 1^1B_2 states were single excitations to LUMO, $4b_2 \rightarrow 2b_1$, $6a_1 \rightarrow 2b_1$, and $1a_2(\text{HOMO}) \rightarrow 2b_1$, respectively. As in the triplet states, the double excitations strongly mixed as main configuration, as seen in Table 1. The 2^1A_1 state was dominated by the double excitations to LUMO: $(6a_1)^2 \rightarrow (2b_1)^2$ and $(4b_2)^2 \rightarrow (2b_1)^2$. These large contributions from the doubles reflect the quasi-degenerate nature in the ground state of ozone.

In Table 4, the present results are compared with the experimental data [1] and other previous theoretical results [4–8,10,11,24,51]. We briefly summarize the previous calculations. The MRMP calculation [8] used the cc-pVTZ basis set augmented with the diffuse functions (1s1p1d). The CASPT2 calculation [7] used ANO [4s3p2d1f] basis set. The reference CASSCF calculations for the MRMP and CASPT2 calculations used all valance active space. The MCLR [5] and EOM-CCSDT-3 [11] calculations was performed with TZ2P level basis. Three MRD-CI calculations published in 1978 [4], 2002 [24], and 2003 [51] used DZP basis set which included the bond polarization and Rydberg functions, TZVP plus Rydberg basis set [3s2p2d], and aug-cc-pVTZ respectively. FSMRCC [6,10] calculations used DZP basis set. In all these theoretical results, the three triplet states were calculated to be lower than the four low-lying singlet states. The 1^1B_2 state was assigned to the Hartley band at 4.9 eV, which lies in the energy region much higher than the other three low-lying singlet states. However, as shown in Table 4, the singlet excitation energies for the 1^1A_2 and 1^1B_1 states were calculated to be very close to each other. Therefore, there are different assignments, depending on the method and the basis set used. The same is also seen in the triplet excitation energy for the 1^3B_1 and 1^3B_2 states.

In our result, the excitation energy of the 1^1B_1 state (2.18 eV) is slightly lower than that of the 1^1A_2 state (2.21 eV). Since the 1^1A_2 state is optically forbidden, the 1^1B_1 state is preferably assigned to the experimental peak

Table 4
Vertical excitation energy (eV) of valence singlet and triplet excited states of ozone calculated by the MEG4/EX-MEG4 method and other theoretical methods

State	Present[a]	Exptl.[b]	Previous theoretical studies								
			CASPT2(g_2)[c]	MRMP[d]	MCLR[e]	FSMRCC[f]	FSMRCC[g]	EOM-CCSDT3[i]	MRD-CI[j]	MRD-CI[h]	MRD-CI[k]
Singlet states											
2^1A_1	4.38		4.33					5.95	4.39	3.60	4.24
1^1A_2	2.21	~1.6	2.03	1.88	2.14	2.17	1.87	2.23	2.27	1.72	
1^1B_1	2.18	2.1	2.11	1.97	2.17	2.13	1.98	2.29	2.15	1.95	
1^1B_2	5.27	4.9	4.69	4.81	5.10	5.52	5.32	5.21	4.85	4.97	4.99
Triplet states											
1^3A_2	2.07	–	1.77	1.65	1.81	1.95	1.68	1.94	2.15	1.44	
1^3B_1	1.77	–	1.62	1.51	1.66	1.62	1.53	1.79	1.85	1.59	
1^3B_2	1.78	–	1.67	1.71	1.14	1.37	1.18	1.64	1.46	1.20	

[a] MEG4/EX-MEG4 result with TZ + Rydberg basis set. Reference function is $-0.92(\text{HF}) + 0.37((1a_2)^2 \rightarrow (2b_1)^2) - 0.12((1b_1) \rightarrow (2b_1))$.
[b] Ref. [1].
[c] Ref. [7]. ANO [4s3p2d1f] basis set.
[d] Ref. [8]. cc-pVTZ + diff. [1s1p1d].
[e] Ref. [5]. POL1 [5s3p2d] basis set.
[f] Ref. [6]. Huzinaga-Dunning (9s5p/1d)/[4s2p1d] basis set.
[g] Ref. [10]. DZP basis set.
[h] Ref. [4]. Dunning (10s5p)/[4s2p] + Ryd. [1s1p] (central oxygen) + Bond pol. [1s] (each bond).
[i] Ref. [11]. POL1 [5s3p2d] basis set.
[j] Ref. [24]. TZVP for triplet, TZVP + Rydberg basis set [3s2p2d] for singlet.
[k] Ref. [51]. aug-cc-pVTZ basis set.

at 2.1 eV which has the intensity much larger than the peak around 1.6 eV [50]. More elaborate calculations using larger basis set would be necessary for obtaining a conclusive result about the ordering of these states.

In the previous studies [4,5,7,8,10,11], the 1^1A_2 state was calculated to have smaller excitation energy than the 1^1B_1 state, although the difference was very small as seen in Table 4. For the 2^1A_1 state, which produced by the two-electron process, the present EX-MEG4 calculation gave 4.38 eV for the excitation energy, which is close to the CASPT2 and the recent MRD-CI results [7,24,51], while the previous MRD-CI excitation energy was very small, 3.60 eV. The EOM-CCSDT-3 gave much higher excitation energy of 5.95 eV, which could be due to the lack of quadruple excitation operators in the wave function. For the 1^1B_2 state, the present calculation gave the excitation energy of 5.27 eV. This state was assigned to the Hartley band observed at 4.9 eV [4,5,7,8,11].

As shown in Table 1, the excitation energy calculated by the EX-MEG4 method showed only minor changes with the different number of the reference functions. Even EX-MEG4 (1 Ref.) result, which is identical to the single-reference SAC-CI general-*R* calculation, was comparable to the EX-MEG4 (2 and 3 Ref.) calculations. The previous EOM-CCSDT-3, single-reference coupled-cluster including triples, calculation [11], also gave the excitation energy similar to the present result for the one-electron excited states. This is probably due to the projection space, $\langle\Phi_0|$ as in the ionized states. Because the low-lying excited states were excitations to LUMO, the projection space becomes almost equivalent to that of the SAC-CI general-*R* method (EX-MEG4 (1 Ref.)).

$$\langle\Phi_0|\widehat{E}^a_j = \langle 0|(g_0 + g^{aa}_{ii}\widehat{G}^{aa}_{ii})\widehat{E}^a_j = g_0\langle 0|\widehat{E}^a_j. \quad (3)$$

The indices *i* and *a* represent HOMO and LUMO, respectively, and *j* is arbitrary occupied orbital.

4. Conclusion

The MEG4/EX-MEG4 method has been applied to the singlet and triplet excited states and the ionized states of ozone. The ground electronic structure of ozone has a bi-radical character and the MEG4 method significantly improved the correlation energy over the SAC method. This is because the HOMO–LUMO double excitation operator was included in the multi-reference configurations of the wave function. The ionization spectrum was also improved by 0.07–0.23 eV, and the experimental spectrum was reproduced in a wide energy range from the outer-valence to the high-energy inner-valence regions up to 28 eV. For the satellite peaks, our calculation supported the previous assignments for the peak A and 4. New assignments were proposed for the peaks 5 and 6 in the experimental spectrum [15]. We have also given new assignments for the peaks B, C, and D lying in the higher-energy region of peak 6.

The present results for singlet and triplet excited states are comparable with the other recent theoretical results. However, the 1^1A_2 and 1^1B_1 states were calculated to be very close to each other and the same for the 1^3B_1 and 1^3B_2 states.

The MEG4/EX-MEG4 method can describe well quasi-degenerate electronic structures and give nice agreements with the experimental data, which is better than those obtained with the SAC-CI general-*R* method.

Acknowledgements

This study has been supported by the Grant for Creative Scientific Research from the Ministry of Education, Science, Culture, and Sports of Japan and partly by Matsuo Foundation.

References

[1] J.I. Steinfeld, S.M. Adler-Golden, J.W. Gallagher, J. Phys. Chem. Ref. Data 16 (1987) 911.
[2] D.W. Arnold, C. Xu, E.H. Kim, D.M. Neumark, J. Chem. Phys. 101 (1994) 912.
[3] S.M. Anderson, P. Hupalo, K. Mauersberger, J. Chem. Phys. 99 (1993) 737.
[4] K.-H. Thunemann, S.D. Peyerimhoff, R.J. Buenker, J. Mol. Spect. 70 (1978) 432.
[5] D. Nordfors, H. Ågren, H.J.Aa. Jensen, Int. J. Quantum Chem. 40 (1991) 475.
[6] M. Barysz, M. Rittby, R.J. Bartlett, Chem. Phys. Lett. 193 (1992) 373.
[7] P. Borowski, M. Fülscher, P.-Å. Malmqvist, B.O. Roos, Chem. Phys. Lett. 237 (1995) 195.
[8] T. Tuneda, H. Nakano, K. Hirao, J. Chem. Phys. 103 (1995) 6520.
[9] A.J. McKellar, D. Heryadi, D.L. Yeager, J.A. Nichols, Chem. Phys. 238 (1998) 1.
[10] N. Vaval, S. Pal, J. Chem. Phys. 111 (1999) 4051.
[11] J.D. Watts, R.J. Bartlett, Spectrochim. Acta A 55 (1999) 495.
[12] D.C. Frost, S.T. Lee, C.A. McDowell, Chem. Phys. Lett. 24 (1974) 149.
[13] C.R. Brundle, Chem. Phys. Lett. 26 (1974) 25.
[14] J.M. Dyke, L. Golob, N. Jonathan, A. Morris, M. Okuda, J. Chem. Soc. Faraday Trans. 270 (1974) 1828.
[15] S. Katsumata, H. Shiromaru, T. Kimura, Bull. Chem. Soc. Jpn. 57 (1984) 1784.
[16] A. Mocellin, K. Wiesner, F. Burmeister, O. Björneholm, A. Naves de Brito, J. Chem. Phys. 115 (2001) 5041.
[17] K. Wiesner, R.F. Fink, S.L. Sorensen, M. Andersson, R. Feifel, I. Hjelte, C. Miron, A. Naves de Brito, L. Rosenqvist, H. Wang, S. Svensson, O. Björneholm, Chem. Phys. Lett. 375 (2003) 76.
[18] H. Couto, A. Mocellin, C.D. Moreira, M.P. Gomes, A. Naves de Brito, M.C.A. Lopes, J. Chem. Phys. 124 (2006) 204311.
[19] H. Basch, J. Am. Chem. Soc. 97 (1975) 6047.
[20] P.J. Hay, T.H. Dunning Jr., W.A. Goddard III, J. Chem. Phys. 62 (1975) 3912.
[21] L.S. Cederbaum, W. Domcke, W. von Niessen, W.P. Kraemer, Mol. Phys. 34 (1977) 381.
[22] N. Kosugi, H. Kuroda, S. Iwata, Chem. Phys. 58 (1981) 267.
[23] P. Decleva, G.D. Alti, A. Lisini, J. Chem. Phys. 89 (1988) 367.
[24] M.H. Palmer, A.D. Nelson, Mol. Phys. 100 (2002) 3601.
[25] T. Schmelz, G. Chambaud, P. Rosmus, H. Köppel, L. Cederbaum, H.-J. Werner, Chem. Phys. Lett. 183 (1991) 209.
[26] H. Müller, H. Köppel, L.S. Cederbaum, T. Schmelts, G. Chambaud, P. Rosmus, Chem. Phys. Lett. 197 (1992) 599.

[27] H. Müller, H. Köppel, L.S. Cederbaum, J. Chem. Phys. 101 (1994) 10263.
[28] C. Woywod, M. Stengle, W. Domcke, J. Chem. Phys. 107 (1997) 7282.
[29] H. Flöthmann, C. Beck, R. Schinke, C. Woywod, W. Domcke, J. Chem. Phys. 107 (1997) 7296.
[30] H. Flöthmann, R. Schinke, C. Woywod, W. Domcke, J. Chem. Phys. 109 (1998) 2680.
[31] H. Nakatsuji, K. Hirao, J. Chem. Phys. 68 (1978) 2053.
[32] H. Nakatsuji, Chem. Phys. Lett. 59 (1978) 362;
H. Nakatsuji, Chem. Phys. Lett. 67 (1979) 329;
H. Nakatsuji, Chem. Phys. Lett. 67 (1979) 334.
[33] H. Nakatsuji, Acta Chim. Hung. 129 (1992) 719.
[34] H. Nakatsuji, in: J. Leszcynski (Ed.), Computational Chemistry – Review of Recent Trends, vol. 2, World Scientific, Singapore, 1997, p. 62.
[35] M. Ehara, M. Ishida, K. Toyota, H. Nakatsuji, in: K.D. Sen (Ed.), Reviews in Modern Quantum Chemistry, World Scientific, Singapore, 2002, p. 293.
[36] H. Nakatsuji, J. Chem. Phys. 83 (1985) 713.
[37] H. Nakatsuji, J. Chem. Phys. 95 (1991) 4296.
[38] H. Nakatsuji, J. Chem. Phys. 83 (1985) 5743.
[39] H. Nakatsuji, J. Chem. Phys. 94 (1991) 6716.
[40] T. Tanaka, Y. Morino, J. Mol. Spect. 33 (1970) 538.
[41] T.H. Dunning Jr., J. Chem. Phys. 55 (1971) 716.
[42] H. Nakatsuji, Chem. Phys. 75 (1983) 425.
[43] S. Süzer, S.T. Lee, D.A. Shirley, Phys. Rev. A 13 (1976) 1842.
[44] R.I. Martin, D.A. Shirley, J. Chem. Phys. 64 (1976) 3685.
[45] M. Dupuis, A. Farazdel, MOTECC-91, Center for Scientific and Engineering Computations, IBM.
[46] H. Nakatsuji, Program System for the EGWF and EX-EGWF Methods Applied to Molecular Ground, Excited, Ionized, and Electron Attached States (General program for MR-SAC and MR-SAC-CI Methods), 1990.
[47] K. Hirao, J. Chem. Phys. 95 (1991) 3589.
[48] T.H. Dunning Jr., J. Chem. Phys. 90 (1989) 1007.
[49] A. Banichevich, S.D. Peyerimhoff, J.A. Beswick, O. Atabek, J. Chem. Phys. 96 (1992) 6580.
[50] R.J. Celotta, S.R. Mielczarek, C.E. Kuyatt, Chem. Phys. Lett. 24 (1974) 428.
[51] Z.-W. Qu, H. Zhu, R. Schinke, Chem. Phys. Lett. 377 (2003) 359.